

**Large-Scale Electricity Storage Utilizing Reversible Solid Oxide Cells Combined With Underground Storage of CO₂ and CH₄**

Journal:	<i>Energy & Environmental Science</i>
Manuscript ID:	EE-ART-05-2015-001485.R1
Article Type:	Paper
Date Submitted by the Author:	22-Jun-2015
Complete List of Authors:	Jensen, Søren; Technical University of Denmark, Energy Conversion and Storage Graves, Christopher; Technical University of Denmark, Mogensen, Mogens; Technical University of Denmark, Wendel, Christopher; Colorado School of Mines, Mechanical Engineering Braun, Robert; Colorado School of Mines, Mechanical Engineering Hughes, Gareth; Northwestern University, Materials Science and Engineering GAO, ZHAN; Northwestern University, Materials Science Barnett, Scott; Northwestern University, Materials Science and Engineering

ARTICLE

Large-Scale Electricity Storage Utilizing Reversible Solid Oxide Cells Combined With Underground Storage of CO₂ and CH₄

Cite this: DOI: 10.1039/x0xx00000x

Received 00th January 2012,
Accepted 00th January 2012

DOI: 10.1039/x0xx00000x

www.rsc.org/

S. H. Jensen^a, C. Graves^a, M. Mogensen, C. Wendel^b, R. Braun^b, G. Hughes^c, Z. Gao^c and S. A. Barnett^c,

Electricity storage is needed on an unprecedented scale to sustain the ongoing transition of electricity generation from fossil fuels to intermittent renewable energy sources like wind and solar power. Today pumped hydro is the only commercially viable large-scale electricity storage technology, but unfortunately it is limited to mountainous regions and therefore difficult to expand. Emerging technologies like adiabatic compressed air energy storage (ACAES) or storage using conventional power-to-gas (P2G) technology combined with underground gas storage can be more widely deployed, but unfortunately for long-term to seasonal periods these technologies are either very expensive or provide a very low round-trip efficiency. Here we describe a novel storage method combining recent advances in reversible solid oxide electrochemical cells with sub-surface storage of CO₂ and CH₄, thereby enabling large-scale electricity storage with a round-trip efficiency exceeding 70% and an estimated storage cost around 3 ¢/kWh, i.e., comparable to pumped hydro and much better than previously proposed technologies.

Introduction

Increasing the utilization of renewable wind and solar sources in electricity grids will require increased use of storage to manage the substantial fluctuations in both supply and demand.^{1,2} The overall future storage need is estimated to be 15-20% of the annual load, i.e. 2-3 month of storage.³ Existing electricity storage technologies have considerable challenges when storage is needed for several months, because of either low efficiency, high cost, or the large scale involved.^{4,5} The storage method described here combines recent advancements in reversible solid oxide electrochemical cell (ReSOC) technology⁶⁻¹⁰ with known gas storage technology,^{11,12} thereby enabling storage of 3 months of electricity supply, i.e. comparable to pumped hydro in capacity, cost, and efficiency.^{1,4}

ReSOCs can use electricity to convert H₂O and CO₂ into H₂, CO and O₂ ("electrolysis mode") and produce power by the reverse process ("fuel cell mode"). The electrolytic conversion is very endothermic (consumes heat) and the reverse conversion is very exothermic (produces heat), which unfortunately implies a considerable heat loss and a low round-trip efficiency. However, by operating the ReSOCs at relatively low

temperature and high pressure the produced CO and H₂ can be catalytically converted to a CH₄-rich gas inside the cell.¹³ The heat generated by the exothermic CH₄ formation can be used by the endothermic CO and H₂ formation, thereby minimizing heat losses and optimizing round-trip efficiency.^{14,15} Cost-effective storage of H₂O in reservoirs,¹⁶ and underground storage of pressurized CO₂ and CH₄¹² enable large energy capacity and long storage times. Our analysis shows that electricity arbitrage using the ReSOC system could become profitable in the future when the prevalence of renewable electricity sources leads to large spreads in electricity prices.¹⁷

Results and Discussion

Fig. 1 shows the proposed storage system schematically. The main components are the electrochemical conversion module consisting of a stack of ReSOCs, underground caverns for storing a CH₄-rich gas and a CO₂-rich gas, and a water reservoir. The ReSOC is represented in a simplified way as an electrode/electrolyte/electrode tri-layer, and the relevant simplified electrochemical reactions are given at each electrode. Additional balance-of-plant (BOP) needed for gas/water processing, not shown in Fig. 1, includes heat exchangers for

efficiently heating/cooling gases as they enter/exit the ReSOC; compressors/expanders for pressurizing/expanding gases between ambient air, and a water condenser for removing steam from, and an evaporator for adding steam to, the gases. A detailed diagram of the system including BOP is given in the Electronic Supplementary Information† (ESI), see Fig. S1.

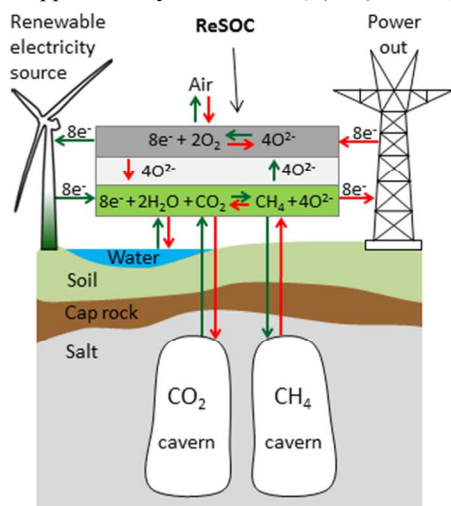


Fig. 1. Schematic diagram of the proposed large-scale electricity storage system. When storing renewable electricity (Electrolysis mode) the reversible solid oxide cell (ReSOC) converts $\text{CO}_2 + \text{H}_2\text{O}$ into CH_4 , by extracting oxygen (green lines). The process is reversed (red lines) when producing electricity on demand (fuel cell mode). Storage caverns and reservoirs are also shown.

The complete energy storage cycle can be described as follows. During electricity storage (electrolysis mode), compressed CO_2 -rich gas is expanded, mixed with H_2O , heated, and then introduced into the ReSOC, which uses electrical power to extract oxygen and produce a CH_4 -rich fuel gas; water is condensed and removed from this gas upon cooling, and then CH_4 is finally compressed for storage. During electricity production (fuel cell mode), compressed CH_4 -rich fuel gas is expanded, mixed with H_2O , heated, and then introduced into the ReSOC, which oxidizes the fuel to generate power and produce a $\text{CO}_2/\text{H}_2\text{O}$ -rich mixture; the H_2O is condensed out upon cooling, and the CO_2 -rich gas is compressed for storage.

Many system components can be shared between both SOFC mode (discharge) and SOEC mode (charge). In each mode of operation, reactant gas is discharged from the pressurized storage cavern, expanded to the ReSOC stack operating pressure, humidified, and preheated. Within the ReSOC stack, reactant species are electrochemically converted to either produce power or fuel. In SOFC mode, power is produced when the reactant fuel species are electrochemically oxidized to H_2O and CO_2 . In SOEC mode, power is supplied to electrochemically reduce H_2O and CO_2 to CH_4 , H_2 , and CO fuel constituents. The gas leaving the ReSOC stack is cooled as it preheats the inlet gas, and undergoes dehumidification in the condenser; additional cooling takes place with intercoolers

during gas compression to the storage pressure. Water to/from evaporator/condenser is stored in the H_2O reservoir.

In both operating modes, air is supplied to the ReSOC stack which must be compressed and preheated from ambient conditions. In SOFC mode, air acts as a heat sink for the exothermic oxidation reactions. In SOEC mode, air is used as a sweep gas to reduce the oxygen partial pressure at the anodes in the ReSOC stack, thereby promoting oxygen transport away from the electrode, which in turn, reduces the electrical power required to ‘charge’ the energy storage system. The SOEC mode airflow also acts as a heat sink since the SOEC stack is operated exothermally due to the internal methanation reaction. A high temperature ejector is used to recycle exhausted air to reduce size, cost and energy loss in the air processing components. The hot, pressurized air exhausted from the stack is used to preheat reactant streams and is expanded through turbines to recuperate some of the power required by the compressors.

The proposed method is similar to that proposed earlier by Bierschenk *et al.*,¹⁵ but introduces new concepts that are critical to making this a viable large-scale electricity storage technology. Paramount among these are 1) pressurized and intermediate temperature operation of the ReSOC in order to produce a methane-rich product, 2) coupling with low-cost, underground, pressurized storage and 3) condensation of H_2O .

System round-trip efficiency is defined as the ratio of the energy generated from discharging the system to the energy required in charging the system; its value is impacted by both the efficiency of conversion in the ReSOC stack (overpotential) and auxiliary power either consumed or produced by the turbomachinery in the BOP. More specifically, the overall roundtrip system efficiency, η_{RT} , is defined as the quotient of the net energy generated in SOFC mode and the total energy supplied in SOEC mode as given below,

$$\eta_{\text{RT}} = (V_{\text{SOFC}} \cdot q_{\text{SOFC}} - E_{\text{BOP,SOFC}}) / (V_{\text{SOEC}} \cdot q_{\text{SOEC}} + E_{\text{BOP,SOEC}}) \quad (1)$$

where q_{SOFC} and q_{SOEC} are the total charge transferred across the electrolyte and $E_{\text{BOP,SOFC}}$ and $E_{\text{BOP,SOEC}}$ are the total BOP energy required during SOFC mode and SOEC mode, respectively. The auxiliary energy associated with the BOP includes parasitic power needed to drive compressors, as well as any other forms of energy entering the system, such as fuel or thermal energy via process heating streams. For repeatable and self-sustaining energy storage, the system must be eventually re-charged to the original state, requiring that the charge transfer is equal in each operating mode (i.e. $q_{\text{SOFC}} = q_{\text{SOEC}}$)*.

*The charge transfer in SOFC mode, for example, is defined as $q_{\text{SOFC}} = i_{\text{SOFC}} \cdot t_{\text{SOFC}}$, where i_{SOFC} is the current and t_{SOFC} is the operating duration in SOFC mode. Thus a longer operating duration in one mode allows a lower current (i.e., higher efficiency) because $i_{\text{SOFC}} \cdot t_{\text{SOFC}} = i_{\text{SOEC}} \cdot t_{\text{SOEC}}$.

To achieve high round-trip efficiency, thermally integrating the system components is of key importance such that process gas heating and cooling requirements are fully satisfied. For example, steam generation in SOEC mode is accomplished with heat exchange from the hot air exhaust. Also, the products from the ReSOC stack during SOFC mode have a high concentration of steam that must be condensed out prior to compressing the gas stream to storage pressure. Some of the heat rejection required in the condenser is provided by the low temperature evaporator, however additional cooling is required by ambient airflow as shown with the air blower in Fig. S1. Additional information on modeling system components is provided in the ESI.

As noted above, during electrolysis mode (charging), oxygen is extracted from the gas entering the ReSOC – moving to the left on the blue dashed line in the C-O-H composition diagram in Fig. 2A. During fuel cell mode (discharging), oxygen is added – moving to the right. A C/H composition ratio of 1/5.67 was chosen to avoid formation of solid carbon which can destroy the fuel electrode (expected in the region to the upper left in Fig. 2A). The oxygen content used in the storage cycle ranges from about 4% to 40%, as indicated by the points on the blue line. Deleterious processes associated with complete reactant conversion (e.g., nickel catalyst oxidation, reactant starvation) are avoided by setting the oxygen contents so that the gas mixture is neither fully oxidized nor fully reduced within the ReSOC. These compositions also allow a relatively wide range of oxygen contents in order to maximize energy storage capacity.

Fig. 2B shows the predicted equilibrium gas constitutions, for an operating temperature of 650 °C and pressure of 20 bar, versus oxygen content. Prior studies suggest that typical Ni-based ReSOC electrodes are sufficiently catalytic that the gas mixtures approach reasonably close to these predicted equilibrium constitutions.^{15,18} The gas that exits the ReSOC during fuel cell mode is mainly H₂O with some CO₂ and H₂ (shown as the blue dot on the right of Fig 2A at about 40% oxygen) whereas the gas that exits the ReSOC during electrolysis mode is mainly CH₄ with smaller amounts of H₂ and H₂O (shown as the red dot on the left of Fig 2A at about 4% oxygen). After the H₂O is condensed out upon cooling, this latter gas is rich in CH₄ (58%) with substantial H₂ (40%). This mixture has an energy density greater than 70% (based on higher heating value) of that of pure methane.

In general, the equilibrium methane concentration in the gas exiting the ReSOC in electrolysis mode increases with increasing pressure, decreasing temperature and increasing the C/H ratio. This is exemplified in Fig 3 using ThermoCalc, the SSUB3 database and the POLY_3 Equilibrium Calculation Module to calculate the equilibrium gas constitution. The methane concentration as a function of pressure is shown in Fig. 3A. From 20 bar to 50 bar the increase in methane content is fairly limited, increasing ~2%. In the case depicted with a

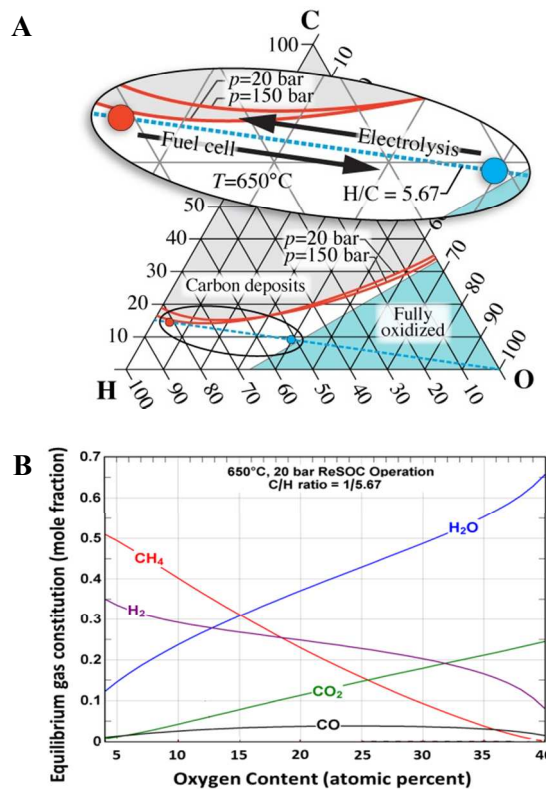


Fig. 2. ReSOC operating conditions (A) C-O-H composition triangle showing the range of gas compositions for the proposed storage cycle, with a C/H ratio of 1/5.67, and oxygen content ranging from 4% to 40%. Also shown are the regions where the gas is fully oxidized (blue), and where carbon deposition is expected (grey) for a temperature of 650 °C and pressures of 20 and 150 bars. (B) Predicted equilibrium gas constitution versus oxygen content, showing how the gas constitution is expected to change as it moves through the ReSOC for an operating temperature of 650 °C and a pressure of 20 bar.

C/H ratio of 1/5.67 and 650 °C, coking is expected to occur at pressures below 15 bar. The C/H ratio also affects the methane concentration as shown in Fig. 3B. In the given example, an increase of 5% methane is obtained when increasing the C/H ratio from 1/6 to 1/5.55. This must be balanced with the risk of coking as more carbon is introduced. At 650 °C and 20 bar, coking will start to occur at a H/C ratio of 5.5. The methane content as function of temperature is shown in Fig 3C. The methane content raises ~3.5% when decreasing the temperature from 650 °C to 450 °C and coking becomes an issue above 675 °C assuming a C/H ratio of 1/5.67 and 20 bar. Additionally, the oxygen content in the outlet gas also affects the methane concentration as exemplified in Fig. 3D. Fig. 3D illustrates that these conditions yield higher CH₄ content in the dry gas (after removal of H₂O) relative to what is presented in Fig. 2B and Fig. 3C, especially for lower temperatures. Regions where coking is expected to occur are indicated with grey shading. The examples on equilibrium gas constitution given in Fig. 3

suggests operating the ReSOC stack at a pressure greater than ~15 bar and a temperature at or lower than ~650 °C in order to avoid coking and to reach a high CH₄ concentration.

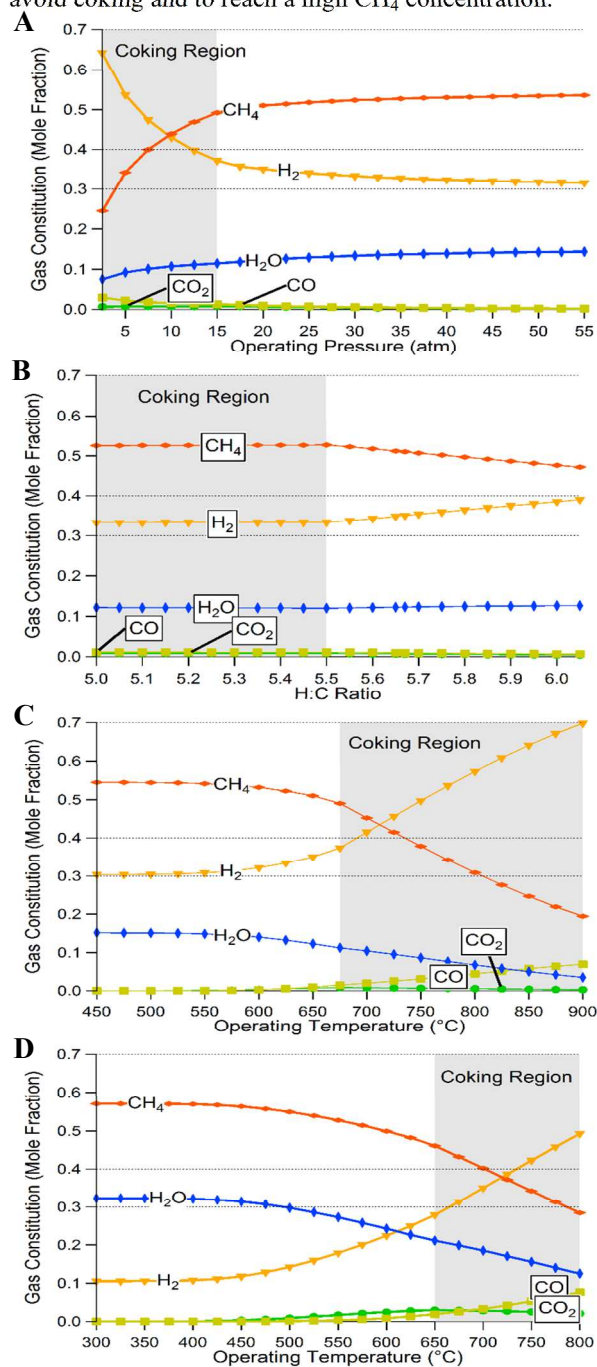


Fig. 3. Gas constitution of the fuel gas as a function of pressure, temperature and H/C ratio. (A) as a function of pressure. (B) H/C ratio. (C) temperature. Reference is 4% oxygen (O), 650 °C and H/C ratio = 5.67. (D) as a function of temperature at a H/C ratio = 5.5, 25 bar pressure, and an oxygen content of 8%.

Recent advances in ReSOC pressure testing supports that 10-20 bar operation is technologically feasible.^{19,20} However, the proposed storage technology is only viable employing ReSOCs that are able to operate with low internal resistance at temperatures $\leq 650^\circ\text{C}$, i.e., with high current density at

relatively low overpotentials. The area specific resistance (ASR) of the ReSOC stack, should preferentially be lower than $0.2 \Omega\text{cm}^2$ to enable high current density to optimize system economy operation without sacrificing system efficiency. This ASR value is relatively low, but not unrealistic. For example, zirconia-electrolyte solid oxide fuel cells²¹ and stacks^{22,23} operating from 750 – 800°C have achieved $0.2 - 0.3 \Omega\text{-cm}^2$ at 1 bar and recently developed solid oxide cells with alternative electrolytes have achieved $0.2 \Omega\text{-cm}^2$ at temperatures from 600 - 650 °C at 1 bar.^{10,24} Also recently developed intermediate-temperature ReSOCs can yield suitable performance. Fig. 4 illustrates test data for such a ReSOC, a button cell with a thin ($\text{La}_{0.9}\text{Sr}_{0.1})_{0.98}\text{Ga}_{0.8}\text{Mg}_{0.2}\text{O}_{3-\delta}$ (LSGM) electrolyte, $\text{La}_{0.6}\text{Sr}_{0.4}\text{Fe}_{0.8}\text{Co}_{0.2}\text{O}_{3-\delta}$ oxygen electrode, and Ni-LSGM fuel electrode, on a $\text{Sr}_{0.8}\text{La}_{0.2}\text{TiO}_{3-\alpha}$ (SLT) support. The ReSOC button cell was fabricated by first a tape casting and laminating porous SLT support, porous LSGM fuel-electrode functional layer, and dense LSGM electrolyte layer, and then co-firing at 1400°C. A composite LSCF-GDC oxygen-electrode functional layer and LSCF current collector were then applied by screen printing and fired at 1100°C. Finally, Ni was wet-chemically infiltrated into the porous SLT support and LSGM functional layer, and then fired at 700°C to produce nano-scale Ni. Fabrication procedures are described in detail elsewhere.²⁵ The cell was tested in air and a 50% H₂ / 50% H₂O fuel mixture, both at 1 bar pressure. Similar cells were reported recently,^{26,27} although the present cells provide a substantial performance improvement over those, with a resistance of only $0.18 \Omega\text{-cm}^2$ at 650 °C. Note that the proposed method utilizes a wide range of fuel mixtures (see Fig. 2B), but we have found that the cell performance does not depend strongly on the fuel composition, with the present H₂/H₂O mixture providing representative results.

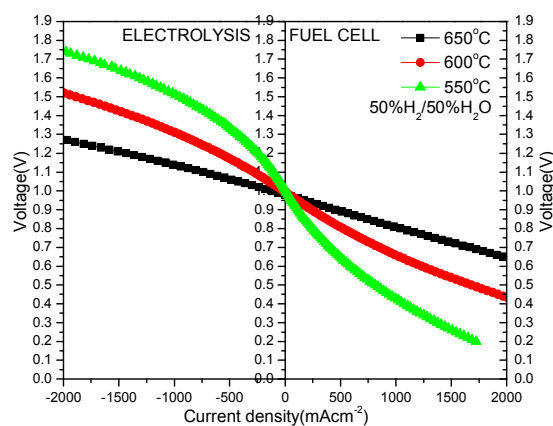


Fig. 4. ReSOC test results. Voltage versus current density at varying operating temperatures, in electrolysis and fuel cell modes, for a button cell with an LSGM electrolyte.

Predicting the actual stack resistance value based on button cell results is complicated. Other researchers also report weak performance dependence on gas composition: Switching from H₂ to CH₄ at 650 °C, 1 bar didn't show a SOFC performance

difference for a NiO/GDC-GDC|GDC|LSCF-GDC button cell (0.56 W/cm^2 for both gasses).²⁸ When increasing the cell size to $5 \text{ cm} \times 5 \text{ cm}$ cells Myung *et al.* observed a decrease in SOFC peak power of less than 15% when switching from H_2 to CH_4 . Increasing pressure from 1 to 10 bar on a Ni/YSZ/YSZ|LSM/YSZ cell ($5 \text{ cm} \times 5 \text{ cm}$) at $750 \text{ }^\circ\text{C}$ decreases the area specific resistance by $\sim 20\%$ when feeding 50% $\text{H}_2\text{O} + 50\% \text{ H}_2$ to the negative electrode and O_2 to the positive electrode.¹⁹ A simulation study of the effect of gas pressure on the cell ASR indicates that increasing pressure from 20 bar to 100 bar will decrease the ASR by less than 15%.²⁹ The cell area-specific resistance shown in Fig. 4 decreases rapidly with increasing cell operating temperature – as mentioned, at $650 \text{ }^\circ\text{C}$ and 1 bar pressure the resistance is $0.18 \text{ } \Omega\text{cm}^2$.

Stack resistance is typically higher than button cell resistance due to current collection losses and depleted gas compositions. Based on the results in Fig. 4 and the above arguments, a stack resistance of $0.2 \text{ } \Omega\text{cm}^2$ at $650 \text{ }^\circ\text{C}$ and 20 bar is a reasonable assumption for the system simulation. Further improvements in the cells will be helpful to allow low resistance at lower temperature and thereby access operating conditions that yield higher methane content (Fig. 3D). In the system simulation presented below, the ASR was taken to be *independent* of temperature and pressure to help illustrate system parametric effects without the complication of a varying ASR. Previously developed ReSOC stack and system models^{14,30-32} are adapted to predict performance of the presented storage system.

System-level simulation was carried out to identify attractive system designs and to enable prediction of realistic round-trip storage efficiencies, here defined as the ratio of the electrical energy (DC power) generated in fuel cell mode to the electrical energy used in electrolysis mode. Fig. 5A depicts total system efficiency as a function of stack pressure for a temperature of $650 \text{ }^\circ\text{C}$, a storage pressure of 160 bar, and three different operating current densities. The curves in Fig. 5A are only shown above a specific pressure value, different for each current density, where it is possible to operate the system without an external heat source. These are the “thermo-neutral” points above which the ReSOC stack produces enough heat, in both operating modes, to maintain its operating temperature and satisfy system gas processing needs that include gas preheat and steam generation. Increasing the pressure shifts the product gas constitution towards an increased CH_4 concentration (Fig. 3), which reduces the thermo-neutral voltage of the electrolysis reaction to values close to the cell equilibrium (Nernst) voltage and thereby decreases the heat requirements.¹⁵ The thermo-neutral point in Fig. 5A shifts to lower pressure with increasing current density because the ReSOC produces more heat at higher currents.

The ReSOC stack efficiency is also shown in Fig. 5A (dashed lines). The difference between stack and system efficiency is caused by the parasitic auxiliary power utilized by the BOP hardware. The stack efficiency varies little with pressure,

because the cell resistance has been assumed independent ($0.2 \text{ } \Omega\text{cm}^2$) of pressure. However, the stack efficiency does decrease with increasing cell current density due to increasing cell overpotentials. System efficiency decreases with increasing pressure for each current density because of increasing parasitic power requirements for gas compression turbomachinery in the air processing BOP, while the decrease in power requirements for fuel processing BOP is relatively small. At 0.8 A/cm^2 and stack pressures near 20 bar, the auxiliary power required by the BOP is either net neutral or can even yield some net power as a result of efficient expansion of the high temperature, high pressure stack exhaust gases.

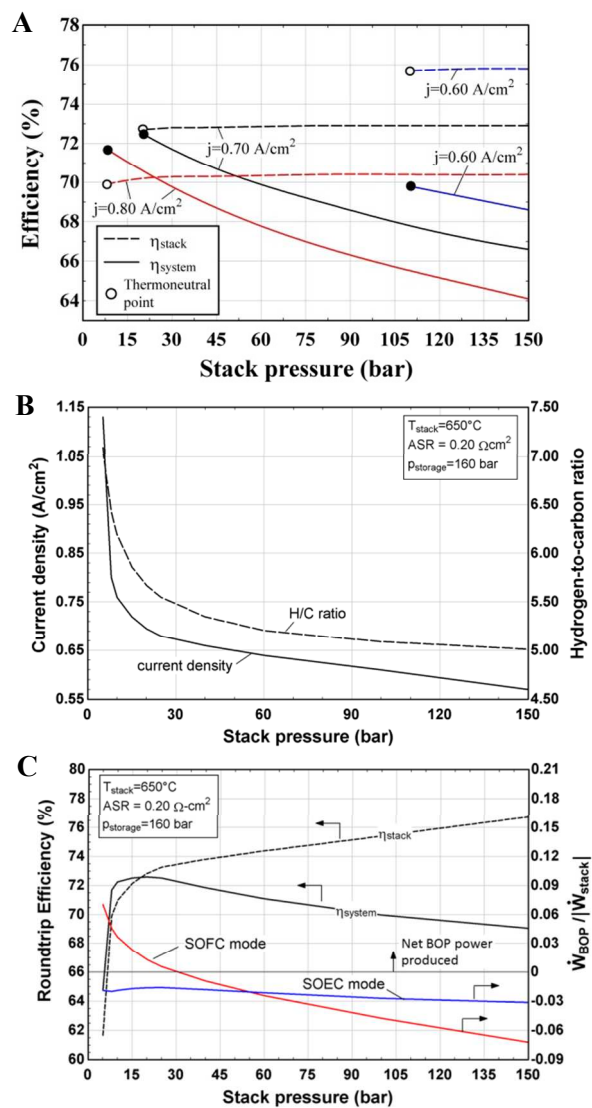


Fig. 5. Influence of operating conditions on system performance. (A) Stack and system round-trip efficiency vs. stack pressure at three different current densities. (B) Minimum current density and H/C ratio vs. stack pressure. (C) Stack and system efficiency (left-axis), and BOP power (\dot{W}_{BOP} , as a fraction of absolute stack electric power, $|\dot{W}_{\text{stack}}|$), in SOEC and SOFC mode (right-axis) vs. stack pressure.

The change in system efficiency and storage energy density can be further understood by considering the influence of ReSOC operating pressure on minimum required current density and fuel composition. The minimum current density and H/C ratio required to operate the system at or slightly above a thermo-neutral condition while remaining outside the carbon-formation regime (Fig 3A), is presented in Fig. 5B.

Maximum roundtrip system efficiency is found at a stack pressure of about 20 bar as shown in Fig. 5C, i.e. at a current density of 0.7 A/cm² (Fig. 5A and 5B). The ReSOC stack efficiency and the BOP power as a function of stack pressure are also depicted in Fig. 5C. Here the stack efficiency increases with increased pressure because the current density required for exothermic SOEC mode operation decreases (Fig 5B), however increased power consumption from the BOP, particularly for air compression, leads to reduced system efficiency at high pressure. At low pressure, the BOP produces net power in discharge mode because of efficient expansion of the high temperature stack exhaust gases, i.e., the exhausted air from the stack can be expanded at higher temperatures while still meeting the required heating processes; however, the net BOP power generation is overcome by a steep decline in stack efficiency at pressures below about 10 bar due to less methanation in SOEC mode.

The system round-trip efficiency also decreases with decreasing ReSOC operation temperature (below 650 °C) due to higher auxiliary power requirements because of reductions in expander power generation from lower gas enthalpy at the expander inlet (not shown in Fig 5.). Additional parametric studies reveal that the system efficiency is maximized around 675°C for a stack pressure of 20 bar.³¹ Above this temperature insufficient methane is generated inside the fuel electrode, which in turn increases the required minimum SOEC operating voltage and thereby decreases efficiency.

While the system efficiency is optimized at an intermediate temperature and stack pressure, energy density (not shown) increases with stack pressure and decreasing stack temperature because more methane, rather than hydrogen, is generated in a pressurized, low-temperature stack. More specifically, although an optimal efficiency is achieved at 20 bar, higher pressure, lower temperature and higher O-content allows more methane and less hydrogen in the generated fuel (Fig. 3). As mentioned above, at 650 and 20 bar and after the H₂O is condensed out upon cooling, the product gas is rich in CH₄ (58%) with substantial H₂ (40%). This is equivalent to a volumetric energy density of ~72% of that of pure CH₄.

To summarize the system simulation, at a stack pressure of ~20 bar, cell current densities of 0.6 – 0.8 A/cm² (with an ASR of 0.2 Ωcm²) will produce sufficient heat to maintain stack temperature and provide gas processing heat requirements (Fig. 5A). This current density is high enough to maintain a reasonable cell cost per kW capacity and low enough to

minimize any cell degradation effects that could compromise lifetime.³³⁻³⁸

Further, round-trip system efficiency peaks above 72% at a stack pressure near 20 bar and a current density of 0.7 A cm⁻² (Fig. 5A and 5C). Importantly, this value is high enough to be competitive with other storage technologies. It should be stressed that the same absolute current density was assumed in both SOEC and SOFC mode. Deviating from this requirement can result in an even higher round-trip efficiency.

Table 1. System cost assumptions

Item	M\$ (\$/kW)	Reference
<u>Installed Capital Cost</u>		
CH ₄ Cavern	36 (144)	12
CO ₂ Cavern	32 (128)	12,39
H ₂ O reservoir	5.8 (23)	16
250 MW ReSOC	50 (200)	40-42
Balance of Stack	0.6 (2.2)	40
Stack Assembly	1.4 (5.7)	40
Air compressor/expander	42 (168)	40
CH ₄ /CO ₂ compressor/expander	21 (86)	40
Recuperators	9.1 (36)	40
Feed water and misc. BOP systems	4.2 (17)	41
Evaporator	7.7 (31)	41
Condenser	4.7 (19)	41
Accessory Electric Plant	20 (80)	40,43
Instrumentation and control	8.5 (34)	40,43
Piping and Valves	8.5 (34)	40
Improvement to site	8.0 (32)	43
Building and structures	8.0 (32)	43
Total plant cost (TPC) sum	269 (1075)	
<u>Fixed O&M</u>		
Labor expenses (8 operating jobs)	3.4 M\$/yr	41,43
<u>Variable O&M</u>		
Maintenance Chemicals	Material, Water, 0.71 ¢/kWh	43
<u>Misc. Estimates</u>		
ReSOC lifetime	5 years	36,38,44-52
System lifetime	20 years	39
Interest rate	5.0 %	
Storage capacity	2000 kWh/kW	Fig. S2B
Volumetric energy density factor	0.72	(20 bar)

In addition to storing large quantities of energy with high efficiency, the ReSOC system must also have a reasonable capital cost – a key criterion for any energy storage technology.⁵³ The storage cost estimate presented here was made assuming a 250 MW ReSOC system and gas caverns large enough to store 500 GWh, or almost 3 months of electricity supply. The cost analysis items are specified in Table 1. The guidelines for economy assessment given by DOE³⁹ was followed in the cost analysis presented below. If not specified, the quoted prices are 2013 prices adjusted for inflation using the US Consumer Price Index.⁵⁴ Details about the individual cost items are provided in the ESI.

To get a rough estimation of the storage cost, we first focus on the investment costs (Installed Capital Cost, Table 1) and use the expression

$$\text{Storage cost (\$/kWh)} = \frac{\text{Capital cost (\$)}}{\text{Energy (kWh)} \cdot \text{Cycles} \cdot \text{Efficiency}} \quad (2)$$

as proposed by Yang *et al.*⁴ In the cost estimation, the system efficiency is taken as 70%. The system can store energy for 2000 hours (500 GWh / 250 MW) which means the numbers of cycles during the system lifetime is 20 years / 2000 hours / 2 = 44 since the system needs to both charge and discharge in one cycle and the system lifetime is estimated to 20 years. The number of cycles for the 250 MW ReSOC stack, Balance of Stack and Stack Assembly is only 11, since the ReSOC lifetime is estimated to 5 years. This means those three cost items are divided with 11 rather than 44 when adding the storage costs of the individual cost items in Table 1 using expression (2). This results in a storage cost estimation of 2.8 ¢/kWh which is lower than CAES and batteries and in some cases comparable with hydropower.⁴ If the lifetime of both system and stack is 20 years, the cost estimation reduces to 1.8 ¢/kWh.

The method proposed by Yang *et al.*,⁴ expression (2), assumes a capacity factor of 100%, i.e. that the system has no idling time. While the storage cost estimation method is desirably simple, in reality the storage system will only operate part of the time, depending on the instantaneous electricity supply and demand.

To estimate the idling time and provide input for a more detailed cost estimation, the optimal revenue from electricity arbitrage (buying and selling power) was estimated using Danish historic hour-by-hour electricity prices⁵⁵ (Historic electricity prices (2006 – 2013) are presented in ESI, Fig. S2A). The arbitrage calculation method is proposed earlier⁵³ and summarized in the ESI. In the calculation a round-trip efficiency of 70% is used. The historic (2006 – 2013) revenue, required storage capacity and selling hours in are presented in ESI, Fig. S2B. In order to achieve the maximum arbitrage in 2008, the ReSOC system should sell electricity for the 2211 hours having the highest electricity prices and buy electricity for the 3159 hours with the lowest electricity prices, which means the ReSOC system capacity factor would be 61% and

that the 250 MW ReSOC system would have an income of 22 M\$ - equivalent to 4.0 ¢/kWh of electricity sold back to the grid. Additionally, the system would require a storage capacity of 1980 hours i.e. slightly below the input of 2000 hours for the calculation above using expression (2).

To provide a more detailed storage cost estimate, Fixed and Variable Operating and Maintenance costs as well as Miscellaneous Estimates are also provided in Table 1 with details for each item given in the ESI. Using these items and a capacity factor of 61%, the storage expense in 2008 is calculated to 42 M\$ - equivalent to 7.7 ¢/kWh sold electricity or an annual expense of 169 \$/kW. These figures were obtained using an annuity loan expression to calculate the total plant cost (TPC) annual expenses, again assuming 5 year stack and 20 year BOP lifetimes. A cost distribution per annum is presented in Fig. 6A.

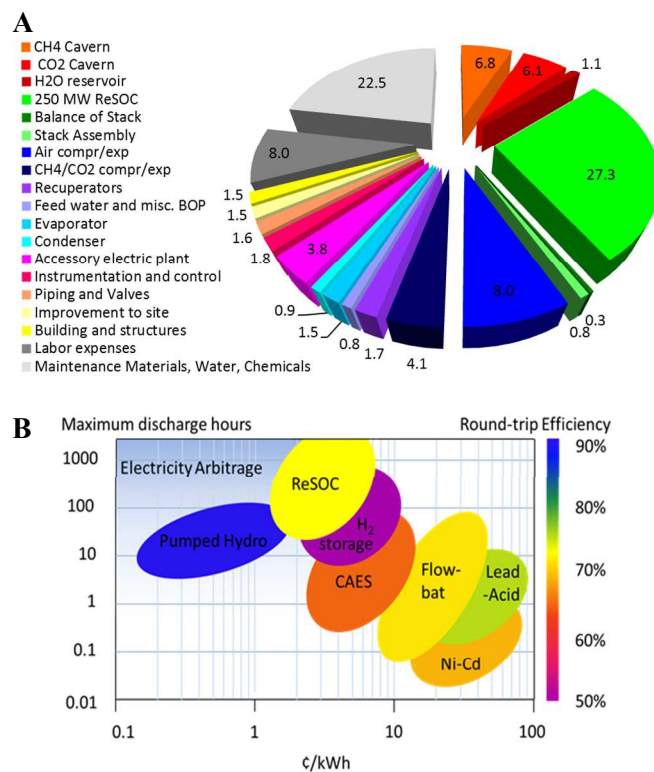


Fig. 6. Cost distribution for the proposed storage system and comparison with other storage technologies. (A) Annual ReSOC storage system expenses in %. (B) Energy storage technologies amended from literature^{1,4} including the ReSOC technology as function of investment cost per kWh per cycle and maximum discharge hours. Efficiency is denoted by the color from purple to blue. Electricity arbitrage is possible for technologies with high efficiency and placed in the upper left part of the graph.

This estimation is fairly complete, including buildings, labor, maintenance, *etc.* Note that the cavern expense is only 14% of the total, meaning that a 50% increase of the maximum storage

capacity would only result in an increase of the total plant cost (TPC) of 7%.

This means the net storage cost in 2008 (balancing storage cost with arbitrage profit) is 3.7 ¢/kWh. However, due to large electricity price fluctuations predicted for 2050¹⁷ (Fig. S2C), which are attributed to increased reliance on highly variable wind power, the system would generate a net *income* of 9.3 ¢/kWh. There are of course considerable uncertainties in these calculations, but they nonetheless show the feasibility that electricity arbitrage using a ReSOC storage system could become profitable in a case where renewable energy sources dominate. Importantly, gas arbitrage and revenue from heat (~30% of the electricity stored with the ReSOC system is lost as heat) sale is not included in the cost estimation. Furthermore, it is reasonable to expect that technological improvements will lead to ReSOC lifetimes exceeding 5 years, which could make the system profitable well before 2050.

The storage cost estimation proposed by Yang *et al.*,⁴ expression (2), is widely used^{1,4} and thus convenient for comparison with other storage technologies (Fig 6B, x-axis). As shown in Fig. 6B the ReSOC system offers a storage cost that is lower than that of CAES, batteries and H₂ storage and, in some cases, is comparable with hydropower.

The only other technologies that can match the combination of high efficiency and low-cost large-scale energy storage, where electricity arbitrage becomes possible are pumped hydro and, to some extent, CAES. These technologies have in common the use of very low cost storage media (*e.g.* water or air) stored in geologic-scale natural formations. However, compared with pumped hydro and CAES, the ReSOC technology has the advantage that the energy storage is chemical, rather than by potential energy, delivering much higher energy density and hence the longer cost-effective storage times. Furthermore, natural gas underground storage and infrastructure needed for the ReSOC technology are widely available compared to pumped hydro, which is limited in capacity by confined geographic availability. Hydrogen storage has been widely considered, but has disadvantages relative to the proposed storage technology due to the lower energy density of hydrogen compared to CH₄ and the low round-trip efficiency.^{15,56,57} The negative consequence of low round-trip efficiency on electricity arbitrage is discussed in ESI and presented in Fig. S2D again using the arbitrage calculation method proposed earlier⁵³ and summarized in the ESI. Finally, secondary and flow batteries utilize relatively more expensive storage media (solid or liquid electrode/electrolyte materials) and hence are more suitable for short-time electricity storage.^{4,58} A comparison of technologies with respect to maximum discharge hours and storage sized is provided in Fig. S3.

Fig. 6B summarizes the key advantages of the proposed ReSOC storage system – the combination of relatively low cost, high round-trip efficiency, and ability to store large quantities of energy for long durations. Much work remains to develop ReSOC energy storage, especially in the area of solid oxide cell development and long-term stability testing.^{38,59-61} However, a

key result from the above analysis is that ReSOC energy arbitrage will be sufficiently profitable such that there should be little or no economic penalty for complementing renewables with the required storage capacity.

Conclusions

The presented analysis describes how a novel storage method combining recent advances in reversible solid oxide electrochemical cells (ReSOC) with sub-surface storage of CO₂ and CH₄, may enable large-scale electricity storage with a round-trip efficiency exceeding 70% and an estimated storage cost around 3 ¢/kWh, excluding possible additional gas arbitrage and profit from heat sale which could reduce storage cost further. With increasing fluctuations in electricity price, the storage system could eventually generate a net income. Thus, it should be possible to simultaneously increase both renewable electricity supply and storage capacity, allowing a continuous decrease in greenhouse gas emissions without sacrificing electricity availability or cost.

Acknowledgements

The authors at DTU Energy Conversion wish to thank the Nordic Energy Research Council (NER) project no. 40000 for financial support. The authors at Northwestern University and Colorado School of Mines gratefully acknowledge financial support from the Global Climate and Energy Project at Stanford University Project under award 51922.

Notes and references

^a Technical University of Denmark.

^b Colorado School of Mines.

^c Northwestern University.

Corresponding author email: shjj@dtu.dk

† Electronic Supplementary Information (ESI) available: [Introduction, System Description, ReSOC System Cost Analysis, Electricity Arbitrage, System Cost Calculation, Fig. S1-3, supplemental references S62-S68]. See DOI: 10.1039/b000000x/

1. B. Dunn, H. Kamath, J. M. Tarascon, *Science*, 2011, **334**, 928.
2. R. M. Dell, D. A. J. Rand, *J. Power Sources*, 2001, **100**, 2.
3. S. Becker *et al.*, *Energy*, 2014, **72** 443.
4. Z. Yang *et al.*, *Chem. Rev.*, 2011, **111**, 3577.
5. B. V. Mathiesen, *et al. Applied Energy* 2015, **145**, 139.
6. J. Yan, H. Matsumoto, M. Enoki, T. Ishihara, *Electrochem. Solid-State Lett.*, 2005, **8**, A38.
7. T. Klemensø *et al.*, *J. Power Sources*, 2011, **196**, 9459.
8. Y.-W. Ju, S. Ida, T. Ishihara, *RSC Advances*, 2013, **3**, 10508.
9. Z. Zhan, D. M. Bierschenk, J. S. Cronin, S. A. Barnett, *Energy & Env. Sci.*, 2011, **4**, 3951.
10. Z. Zhan *et al.*, *RSC Advances*, 2012, **2**, 4075.
11. A. Hosa, M. Esentia, J. Stewart, S. Haszeldine, *Chem. Eng. Research and Design*, 2011, **89**, 1855.

12. A. H. Pedersen, "Evaluation of underground storage of CO₂, O₂ and H₂." (EUDP 64011-0036, Copenhagen, DK, 2011).
13. S. H. Jensen, M. Mogensen in *19th World Energy Congress*. (Sydney, AU, 2004).
14. P. Kazemipoor, R. J. Braun, *Int. J. Hydrogen Energy*, 2014, **39**, 5955.
15. D. M. Bierschenk, J. R. Wilson, S. A. Barnett, *Energy & Env. Sci.*, 2011, **4**, 944.
16. T. Schmidt, D. Mangold, P. A. Sørensen, N. From, in *6th Int. Renew. Energy Storage Conf. and Exhibition*. (Berlin, DE, November 2011).
17. "Energy strategy 2050 – from coal, oil and gas to green energy" (The Danish Ministry of Climate and Energy, Copenhagen, DK, 2011).
18. H. Timmermann, W. Sawady, R. Reimert, E. Ivers-Tiffée, *J. Power Sources*, 2010, **195**, 214.
19. S. H. Jensen, X. Sun, S. D. Ebbesen, R. Knibbe, M. Mogensen, *Int. J. Hydrogen Energy*, 2010, **35**, 9544.
20. J. E. O'Brien *et al.*, "High temperature electrolysis pressurized experiment design, operation, and results" (INL/EXT-12-26891, Idaho National Laboratory, Idaho Falls, US, 2012).
21. Z. Gao, D. Kennouche, S. A. Barnett, *J. Power Sources*, 2014, **260**, 259.
22. B. Borglum, E. Tang, M. Pastula, *ECS Transactions*, 2009, **25**, 65.
23. R. Payne, J. Love, M. Kah, *ECS Transactions*, 2009, **25**, 231.
24. E. D. Wachsman, K. T. Lee, *Science*, 2011, **334**, 935.
25. Z. Gao, S. A. Barnett, *in preparation* (2015).
26. Z. Gao, E. C. Miller, S. A. Barnett, *Advanced Functional Mat.*, 2014, **24**, 5703.
27. E. C. Miller, Z. Gao, S. A. Barnett, *Fuel Cells*, 2013, **13**, 1060.
28. J. H. Myung, H. J. Ko, J. J. Lee, J. H. Lee, S. H. Hyun, *Int. J. Hydrogen Energy*, 2012, **37**, 11351.
29. S. L. Ebbenhøj, PhD thesis, (DTU Energy, Roskilde, Denmark, 2015).
30. P. Kazemipoor, R. J. Braun, *Int. J. Hydrogen Energy*, 2014, **39**, 2669.
31. C. Wendel, P. Kazemipoor, R. J. Braun, *J. Power Sources*, 2015, **276**, 133.
32. Wendel, C. *Design And Analysis Of Reversible Solid Oxide Cell Systems For Electrical Energy Storage*, PhD thesis, Colorado School of Mines (2015).
33. M. Chen *et al.*, *J. Electrochem. Soc.*, 2013, **160**, F883.
34. C. Graves, S. D. Ebbesen, M. Mogensen, *Solid State Ionics*, 2011, **192**, 398.
35. J. Kim *et al.* *Int. J. Hydrogen Energy*, 2013, **38**, 1225.
36. R. Knibbe, M. L. Traulsen, A. Hauch, S. D. Ebbesen, M. Mogensen, *J. Electrochem. Soc.*, 2010, **157**, B1209.
37. V. N. Nguyen, Q. Fang, U. Packbier, L. Blum, *Int. J. Hydrogen Energy*, 2013, **38**, 4281.
38. G. A. Hughes, K. Yakal-Kremiski, S. A. Barnett, *PCCP*, 2013, **15**, 17257.
39. C. K. Ekman, S. H. Jensen, *Energy Conv. and Management*, 2010, **51**, 1140.
40. "Carbon capture and sequestration systems analysis guidelines" (National Energy Technology Laboratory, US, 2005).
41. US Consumer Price Index, www.inflationdata.com (2014).
42. J. Thijssen, "The impact of scale-up and production volume on SOFC manufacturing cost" (National Energy Technology Laboratory, US, 2007).
43. "Cost and performance baseline for fossil energy plants" (DOE/NETL-2007/1281, National Energy Technology Laboratory, US, 2007).
44. J. Warren, S. Das, W. Zhang, in *Fuel Cell Science, Eng. and Techn. Conf.* (San Diego, US, 2012) pp. 25-34.
45. "Integrated gasification fuel cell performance and cost assessment" (DOE/NETL-2009/1361, National Energy Technology Laboratory, US, 2009).
46. M. S. Sohal *et al.*, *J. Fuel Cell Sci. and Techn.*, 2012, **9**, 011017.
47. N. Christiansen, "Development of next generation metal based metal based SOFC technology," (EU FP7 211940, Kgs. Lyngby, DK, 2012).
48. A. Hauch, M. Mogensen, A. Hagen, *Solid State Ionics*, 2011, **192**, 547.
49. S. D. Ebbesen, J. V. T. Høgh, K. A. Nielsen, J. U. Nielsen, M. Mogensen, *Int. J. Hydrogen Energy*, 2011, **36**, 7363.
50. A. Nakajo, F. Mueller, J. Brouwer, J. Van herle, D. Favrat, *J. Power Sources*, 2012, **216**, 434.
51. A. Nakajo, F. Mueller, J. Brouwer, J. Van herle, D. Favrat, *J. Power Sources*, 2012, **216**, 449.
52. M. Chen *et al.*, *Fuel Cells*, 2013, **13**, 638.
53. S. Elangovan, J. Hartvigsen, D. Larsen, I. Bay, F. Zhao, *ECS Transactions*, 2011, **35**, 2875.
54. A. Mortensgaard *et al.*, "GreenSynFuels," (EUDP 64010-0011, Copenhagen, DK, 2011).
55. N. Osada, H. Uchida, M. Watanabe, *J. Electrochem. Soc.*, 2006, **153**, A816.
56. D. Ferrero, A. Lanzini, M. Santarelli, P. Leone, *Int. J. Hydrogen Energy*, 2013, **38**, 3523.
57. U. Bossel, B. Eliasson, G. Taylor, *Cogeneration and Competitive Power J.*, 2003, **18**, 29.
58. C. J. Barnhart, S. M. Benson, *Energy & Env. Sci.*, 2013, **6**, 1083.
59. C. Graves, S. D. Ebbesen, S. H. Jensen, S. B. Simonsen, M. Mogensen, *Nature Mat.*, 2014, **14**, 239.
60. R. Knibbe, A. Hauch, J. Hjelm, S. D. Ebbesen, M. Mogensen, *Green*, 2011, **1**, 141.
61. A. Weber, in *Encyclopedia of Electrochem. Power Sources*, J. Garche, Ed. (Elsevier, Amsterdam, 2009), pp. 120-134.

Today about 2/3 of the global energy consumption is based on fossil fuels and only a minor fraction on renewable energy sources. With a growing consensus among countries that it is time to act and decrease greenhouse gas emissions to avoid uncontrollable climate changes, it is clear that the necessary transition towards renewable-based energy infrastructures has just begun.

However, as intermittent wind and solar power displace fossil fuels, the need for storage to balance the gap between supply and demand increases. This is in particular the case for the electricity sector, where no widely available, energy efficient and cheap large-scale electricity storage technology exists.

The present work analyzes the reversible electrochemical conversion of H_2O and CO_2 to CH_4 inside novel pressurized solid oxide cells combined with subsurface storage of the produced gasses, showing that it should be possible to store about 3 months of electricity (500 GWh) with a round-trip efficiency greater than 70% and a storage cost around 3 ¢/kWh. With the expected rise in arbitrage due to increasing balancing demands and consequent price fluctuations, the technology should eventually become economically viable. In summary, this disruptive new energy storage technology can facilitate a seamless transition towards a fossil-free future.